

Event-Related Potentials and Fast Optical Imaging of Cortical Activity During an Auditory Oddball Task



Manon E. Jaquerod, Ramisha Knight, Alessandro E. P. Villa,
and Alessandra Lintas

1 **Abstract** Event-related potentials (ERP) have been repeatedly used to study the
2 spatiotemporal dynamics of the attentional response in the well-known oddball
3 paradigm. We combined electroencephalography (EEG) with frequency-domain
4 near-infrared spectroscopy (fNIRS) of the frontal cortex to measure neuronal activity
5 with a high spatial and temporal resolution. The aim of this study was to determine
6 the precise chronology of event-related optical signals (EROS) and their consistency
7 with ERPs. In agreement with previous studies, the oddball condition produced larger
8 waveforms for rare (1500 Hz pure tone) with respect to frequent stimuli (1000 Hz),
9 with N1, P2, N2, P3a, and P3b components. At a latency corresponding to the mis-
10 match negativity/N2 wave component, EROS showed the organization of a complex
11 activity in a functional network of frontal areas, with rare tones activating the left
12 premotor dorsal cortex and the left inferior frontal cortex and decreasing the activity
13 of the right superior frontal gyrus. Rare tones elicited also a strong N500 (N400-like)
14 wave component that EROS contributed to localize at the level of the right medial
frontal gyrus by EROS. The simultaneous recording of fNIRS and EEG measure-

M. E. Jaquerod (✉) · A. E. P. Villa · A. Lintas
NeuroHeuristic Research Group, University of Lausanne, Internef 138, Quartier
UNIL-Chamberonne, 1015 Lausanne, Switzerland
e-mail: manon.jaquerod@unil.ch
URL: <http://www.neuroheuristic.org>

A. E. P. Villa
e-mail: alessandra.lintas@unil.ch

A. Lintas
e-mail: alessandro.villa@unil.ch

A. E. P. Villa
LABEX, HEC Lausanne, Faculty of Law, Criminal Justice and Public Administration,
University of Lausanne, Quartier UNIL-Chamberonne, 1015 Lausanne, Switzerland

R. Knight
University of Illinois, 2111 Beckman Institute, 405 North Mathews Avenue,
Urbana, IL 61801, USA
e-mail: rsknight@illinois.edu

© Springer Nature Singapore Pte Ltd. 2021
A. Lintas et al. (eds.), *Advances in Cognitive Neurodynamics (VII)*,
Advances in Cognitive Neurodynamics,
https://doi.org/10.1007/978-981-16-0317-4_18

1

15 ments with high temporal accuracy over the human prefrontal cortex supports the
16 potential for this approach to unravel the functional cortical network involved in
17 cognitive processing.

18 **1 Introduction**

19 A fundamental property of animal behavior is habituation, i.e., the decrement of
20 response with repeated stimulation, which is a necessary process to detect deviant
21 or novel stimuli (Blumstein, 2016; Thompson, 2009). A classical paradigm, called
22 “oddball” paradigm, used to study the responsiveness to a repeated auditory stimulus
23 consists of a long sequence of repetitive identical stimuli (the frequent stimuli) that
24 is replaced with a low probability, and at random, by a different stimulus (the rare
25 stimulus). Brain activity elicited by frequent and rare stimuli has been recorded by
26 electrophysiological means to study the brain processes underlying attention switches
27 to, and involuntary discrimination of, rare among the frequent stimuli. Animal studies
28 showed that responses at the level of the cerebral cortex are associated with attentional
29 circuits that are strongly affected during anesthesia (Apelbaum et al., 1960; Eriksson
30 & Villa, 2005; Ruusuvirta et al., 1996).

31 In humans, the oddball paradigm was implemented in active and passive condi-
32 tions (Näätänen, 1990; Squires et al., 1975). The active condition is an attentional
33 task, such that the participant must attend to all stimuli in order to detect the rare
34 stimuli and generate a motor response, e.g., a key-press. In the passive condition,
35 the participant is usually instructed to ignore all stimuli and to attend other stimuli,
36 usually presented in another sensory modality. Maintaining a goal-directed behavior
37 that requires selective attention, brain responses to the habituation of the frequent
38 stimuli, and the salient perception of rare stimuli may bring insights about reorien-
39 tation of attention. The oddball paradigm has been extensively studied by electroen-
40 cephalography (EEG), i.e., by measuring variations in the electric field at the scalp
41 induced by the summation of mass neuronal firing rates with a millisecond-level
42 of resolution. The selective sensitivity of the technique for brain layers with corre-
43 lated dipoles makes neural activity in sulci far less represented in the EEG signal
44 than neural activity in gyri (Nunez, 1995). Furthermore, the spatial filtering of fields
45 by the head volume conductor implies interdependencies of measurements between
46 electrode sites and strongly restrain the capacity for EEG to depict the precise spa-
47 tial distribution of patterns of activity (Nunez, 1995). The event-related potentials
48 (ERPs) are obtained by averaging, over many trials, the EEG signal variations trig-
49 gered by sensory or behavioral events. Endogenous ERPs are thought to reflect the
50 neurophysiological correlates of cognitive processes.

51 In the oddball paradigm, the auditory stimuli elicited ERPs characterized by sev-
52 eral components (N1, P2, N2, P3) whose latencies and amplitudes differentiated rare
53 from frequent stimuli (Alexander et al., 1994; Michalewski et al., 1986; Näätänen,
54 1990). The N1 wave is generated by a stimulus-driven attention-trigger mechanism
55 (Näätänen & Picton, 1987). A positive component P2 of the ERP is often preced-

ing the negative component N2 at approximately 250 ms after rare stimuli (Goodin et al., 1978). This wave may often be dissociated into an earlier fronto-central N2a component (also known as “mismatch negativity”) and a later, more frontally distributed, N2b component associated with the allocation of attention to the eliciting stimulus in the active oddball condition (Näätänen, 1990; Squires et al., 1975). The mismatch negativity (MMN), characterized by its responsiveness to low probability stimuli even in the passive auditory oddball condition, may underlie the ability to discriminate acoustic differences, a fundamental aspect of sensory perception. The N2 is followed by the P3 (P300) component, with larger amplitude in active than in passive conditions, formed by a fronto-central wave complex N2-P3a that can be dissociated from a temporo-parietal P3b wave (Molnár, 1994; Näätänen, 1990; Polich, 2007; Squires et al., 1975; Verleger, 1988). In addition, at 400–500 ms from stimulus onset, the rare stimuli elicited a slow frontally maximal negativity, referred to as N500 (N400-like) (Gaillard, 1976).

Signals recorded by functional magnetic resonance imaging (fMRI) are associated with the blood-oxygen-level-dependent (BOLD) signal, an hemodynamic indirect measure of neural activity with severe limitations in temporal resolution and with challenging interpretation to make deductions about the nervous system. The activation of spatially limited neuronal populations may not be strong enough to produce significant hemodynamic changes, but still produce a significant ERP wave. Brain imaging with fMRI has been used to localize the brain areas activated during the P3 wave elicited by the oddball paradigm (Linden et al., 1999; McCarthy et al., 1997; Menon et al., 1997). In fMRI studies, the detection of rare stimuli in oddball tasks related to BOLD signal increased in the supramarginal (Horowitz et al., 2002; Mangalathu-Arumana et al., 2012; McCarthy et al., 1997; Menon et al., 1997) and superior temporal gyri (Mangalathu-Arumana et al., 2012; Opitz et al., 1999), in agreement with greater wave amplitude of P3b observed at the temporal/parietal electrode sites of EEG. A significant hemodynamic response was also reported in the frontal lobe, in particular at the level of the middle frontal gyrus (MFG) (Horowitz et al., 2002; McCarthy et al., 1997; Stevens et al., 2005), frontal midline areas (Menon et al., 1997) and the opercular area of the inferior frontal gyrus (IFG), corresponding to Brodmann area 44 (Linden et al., 1999). The ERP response to the oddball paradigm is complex and cannot be reduced to its P3 component. Besides the spatial dependency of its signal on the location of blood vessels, fMRI relies on an indirect correlate of neural activity which is intrinsically too slow to reveal the complexity of neurodynamics. Hence, it is likely that BOLD fMRI signal generation reflects the sustained activity of a large neuronal system triggered by the rare stimuli and that brief synaptic activity, evoked by those stimuli in dynamic neural circuits, might be detectable only with methods characterized by signal-to-response dynamics faster than neurovascular signals.

Transcranial near infrared spectroscopy (NIRS) allows the non invasive differentiation between tissues with different light attenuation or scattering properties and can provide spectroscopic information on the concentrations of chromophores, in particular oxy- and deoxy-haemoglobin, HbO₂ and Hb (Chance et al., 1993; Delpy & Cope, 1997; Gratton et al., 1995; Scholkmann et al., 2014; Strait & Scheutz, 2014;



101 Torricelli et al., 2014). A slow hemodynamic signal, corresponding to cerebral blood
102 oxygenation variations, is measured as a function of near-infrared light propagation
103 through extra-cerebral and cerebral tissue. Both the optical path length and the cere-
104 brospinal fluid layer affect the measurement, but the geometry of the sulci and the
105 boundary between the gray and the white matter have little effect on the detected light
106 distribution (Okada et al., 1997). The NIRS hemodynamic signal, which is similar
107 to the BOLD signal measured by fMRI, is modified by neuronal activity through
108 neurovascular coupling with latencies of several seconds. In addition to the mea-
109 surement of changes in light intensity, fNIRS instruments with a frequency-domain
110 technology of measurement allow the recording of a fast optical signal with a latency
111 in the order of milliseconds (Gratton & Fabiani, 2010). This measurement, made pos-
112 sible by the modulation of light sources at a high radio-frequency (e.g., 110 MHz),
113 is based on a complex function of the tissue absorption and scattering coefficients to
114 include changes in light intensity with distance, phase, and modulation depth changes
115 of intensity-modulated light and the temporal dispersion of light from an ultrashort
116 input light pulse (Gratton et al., 1997; Gratton & Fabiani, 2001; Wolf et al., 2002).
117 Neural activity can be directly detected by fast fNIRS signal through changes in the
118 scattering coefficient of the brain tissue. A change in neuronal cell volume following
119 an action potential discharge is meant to account for subtle, yet measurable, variation
120 in the scattering properties of the tissue (Lee & Kim, 2010; Steinbrink et al., 2000;
121 Villringer & Chance, 1997). Although optical imaging with fast fNIRS signals has
122 the potential for a millimeter-level of spatial resolution, it is limited to brain regions
123 located only few centimeters below the scalp (Gratton et al., 1997).

124 The two main cortical associative auditory pathways include a posterior dorsal
125 stream processing spatial (“where”) information from the posterior superior tempo-
126 ral gyrus (STG) to the parietal cortex, and an anterior ventral stream processing
127 an object (“what”) from the anterior part of STG to IFG (Ahveninen et al., 2006).
128 Both pathways send projections to the prefrontal cortex with dorsal (DLPFC) and
129 ventral (VLPFC) regions involved in different roles during the processing of audi-
130 tory information with high cognitive load (Plakke & Romanski, 2016). Simultaneous
131 recording of ERP and the corresponding NIRS response has recently raised consid-
132 erable interest to complement the study of the spatial distribution of cortical and
133 subcortical activation during oddball and go-nogo tasks. Source localization based
134 on the NIRS slower hemoglobin response showed significant oddball activation in
135 temporal/parietal areas (Kennan et al., 2002) with a gender effect suggesting females’
136 event-categorization process is more efficient than in males (Jausovec and Jausovec,
137 2009), and activation of MFG by tasks that require heavy cognitive processing (Jeong
138 et al., 2018). Stronger hemodynamic responses were reported in the left prefrontal
139 cortex when participants were performing an auditory oddball task under mental
140 stress (Liu et al., 2011), but the response was stronger in the right VLPFC when
141 attending to stimuli that required higher cognitive load and negatively correlated
142 with the level of state anxiety (Tseng et al., 2018). The averaging of optical responses
143 evoked by the repetition of the same stimulus allowed the analysis of event-related
144 transient optical responses based on continuous wave measurements of light intensity
145 (Kubota et al., 2008; Medvedev et al., 2008) and the development of event-related

146 optical signal (EROS) analysis by means of frequency-domain instruments, based
147 on a measurement of phase-shifts of the fast optical signal as the photons migrate
148 through the brain tissue, which is optically modified by neural activation (Gratton
149 & Fabiani, 1998). In passive detection of deviant auditory stimuli, source localiza-
150 tion by EROS reported early activity co-occurring with ERP waves localized in the
151 auditory areas of STG (Rinne et al., 1999) followed by activation of VLPFC in pre-
152 attentive auditory change detection (Tse et al., 2013). At a later latency, consistent
153 with P3 and frontal negativity, EROS data have shown activation in the right MFG
154 (DLPFC) by rare stimuli during an auditory oddball task (Low et al., 2006).

155 In this study, we analyzed ERPs and EROS in the frontal cortex elicited by a passive
156 two-tone auditory oddball discrimination task. The task consisted of a random stream
157 of frequent auditory tones (1000 Hz, $p = 92\%$) or an infrequent oddball auditory tone
158 (1500 Hz, $p = 8\%$) being played at a constant interval of 1600 ms. In this paradigm,
159 attention is directed away from the acoustic stimuli with an explicit instruction to
160 fixate on a white cross centered on a screen. Our EROS analysis was mainly based
161 on changes in the phase delay because it has the advantage of a greater sensitivity for
162 deeper locations and a greater spatial resolution than light intensity measurements
163 (Gratton & Fabiani, 2010). These results indicate that the passive auditory oddball
164 task modulated the brain activity measured by EROS in the frontal cortex within
165 the same time range as EEG measures. The simultaneous recording of fNIRS and
166 EEG measurements with high temporal accuracy over the human prefrontal cortex
167 supports the potential for this approach to unravel the functional network involved
168 in cognitive processing.

169 2 Methods

170 2.1 Participants

171 Ten healthy volunteers participated in the study (mean age = 28.1 years; 6 women).
172 All subjects were right-handed and reported normal hearing and normal or corrected-
173 to-normal vision. Prior to participation, subjects were informed about the procedure
174 and provided signed informed consent for their participation in line with the Decla-
175 ration of Helsinki (World Medical Association, 2013) and the recommendations of
176 ethical and data security guidelines of the University of Lausanne. Two subjects (1
177 male and 1 female) were treated as pilot data and were excluded from the analysis.

178 2.2 Procedure

179 The task consisted of 12 blocks with 120 trials each, following the passive auditory
180 oddball paradigm. Frequent (1000 Hz at occurrence probability $p = 92\%$) and a

181 rare (1500 Hz, $p = 8\%$) computer generated tones, lasting 500 ms, were presented
 182 at approximately 60 dB SPL. Each block consisted of a randomized sequence of
 183 frequent and rare tones where stimuli onsets were separated by 1600 ms. Subjects
 184 were only instructed to watch a white fixation cross in the center of a computer screen
 185 placed horizontally at 65 cm in front of the middle of their eyes. In order to minimize
 186 the noise added by environmental light in the NIRS data, experiments were run with
 187 the lights off and the computer screen background was black.

188 2.3 Electrophysiological Recording

189 Continuous EEG was recorded using 64 scalp Ag/AgCl active electrodes (ActiveTwo
 190 MARK II Biosemi EEG System, BioSemi B.V., Amsterdam, The Netherlands), sam-
 191 pled 1024 Hz and referenced to the linked mastoids. Impedance was kept below
 192 20 k Ω . Electrodes were mounted on a head-cap (10/20 layout, NeuroSpec Quick
 193 Cap) that was modified in order to allow the optical equipment to have direct contact
 194 with the scalp (Fig. 1a). Data were preprocessed and analyzed with the EEGLAB
 195 toolbox (MATLAB, The MathWorks, Inc.) (Delorme & Makeig, 2004). EEG data
 196 were then segmented into epochs using markers. Epochs of the continued data with
 197 visible large movement artifacts were removed from the analysis. A poor EEG signal
 198 from a selected electrode was reconstructed by combining signals from neighbor-

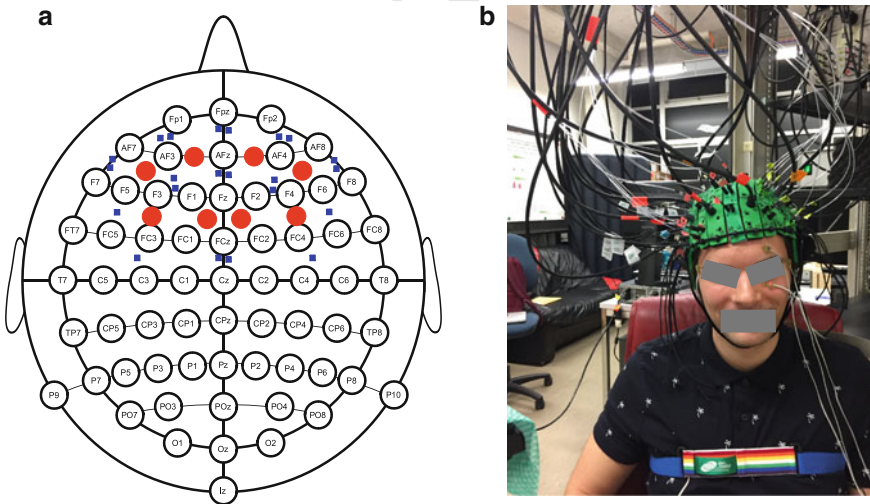


Fig. 1 **a** Schematic representation of the co-localization of the 8 light detectors (red circles) and 22 light sources (blue squares) over prefrontal and premotor areas of the cerebral cortex and the 64-channel electrophysiological setup with the standardized International 10/20 system. **b** The photo-multiplier tube detectors and fiber optic bundles placed over the participant's forehead using a custom-made mounting system

199 ing electrodes using interpolation. The EEG signal was decomposed using an Info-
200 max Independent Component Analysis (ICA) in order to correct eye blink artifacts.
201 Epochs containing visible artifacts after ICA preprocessing were rejected. All epochs
202 kept for the analysis were bandpass filtered between 0.1 and 40 Hz before ERPs were
203 computed.

204 A grand average of the ERP response to the oddball task was calculated by averaging
205 individual participants' ERPs. In this study, we report data recorded at electrode
206 sites Fz, Cz, and Pz, separately for frequent and rare tones. The amplitude was calcu-
207 lated as the voltage difference between a pre-stimulus baseline and the respective
208 peak. The latency was defined by the lag for the ERP wave to reach its peak ampli-
209 tude. We focused our topographic analysis on the time windows corresponding to
210 the main ERP components. The N1/P2 was identified as negative deflection between
211 120 and 150 ms post-stimulus followed by a positive deflection between 170 and
212 230 ms post-stimulus. The MMN/N2 was identified as the largest peak occurring
213 230–260 ms after stimulus presentation, the P3a as the positive deflection between
214 280 and 300 ms and the P3b as the largest peak occurring 350–400 ms after stimu-
215 lus presentation. A large negative wave between 460 and 650 ms post-stimulus
216 characterized the N500 (N400-like) component of the ERP.

217 **2.4 Optical Recording**

218 Optical data were collected using a frequency-domain NIRS system ISS Imagent
219 (Champaign, Illinois, USA) with 8 detectors and 22 frequency-modulated light
220 (830 nm wavelength modulated at 110 MHz) sources. The sources and detectors
221 were co-located with the EEG setup, as shown in Fig. 1a. In the present study, EROS
222 was recorded with source-to-detector distances between 20 and 55 mm. The fiber
223 optic bundles connected to the laser diodes emitting light sources and the fiber optic
224 bundles connected to the detectors (photomultiplier tubes) were held in place using
225 a custom-built head mounting system (Fig. 1b). Detectors amplifiers' were modu-
226 lated at a frequency of 110.005 MHz. Hence, a heterodyning frequency (or cross-
227 correlation frequency) was generated equal to the difference between the frequency
228 modulation of the sources and detectors, i.e. 5000 Hz, thus implying a period of oscil-
229 lation of 0.2 ms. The photomultiplier output current was Fast Fourier Transformed
230 (FFT) on four oscillations (i.e., 0.8 ms). One oscillation was skipped in order to avoid
231 cross-talk between sources, thereby yielding a data acquisition period of 1 ms for
232 each source. Light sources were time multiplexed in a cycle of eight per sampling
233 point, which corresponds to an effective time resolution of 8 ms (i.e., an effective
234 sampling rate 125 Hz). Notice that for each data point, we measured the DC (average)
235 intensity, AC (amplitude) intensity, and relative phase delay.

The locations of each source and detector were digitized with a 3D digitizer (FASTRAK 3Space, Polhemus Inc.). Phase delay measurements in the cross-correlation signal were corrected off-line for phase wrapping and their mean was adjusted to zero. The algorithm described in Gratton and Corballis (1995) was used to remove the pulse artifacts from the signal. Only channels with phase standard deviation smaller than 200 ps were included for further analysis (Gratton et al., 2006). Data were band-pass filtered between 0.1 and 10 Hz before statistical topographical surface projection maps of fast optical signals were computed using the Opt3D software (Gratton, 2000) available at the NeuroImaging Tools & Resources Collaboratory (<https://www.nitrc.org/>). EROS data were spatially filtered with an 8-mm Gaussian kernel and for each subject, contrast, and voxels, t -scores were computed and converted to Z -scores. This approach removes emphasis on larger effects in relation to the smaller effects and was chosen because of our small sample size ($N = 8$).

The regions of interests (ROIs, cf. Table 1 and Fig. 2) were selected on the basis of previous studies on auditory deviance detection. The Talairach space boundaries of our ROIs were kept consistent with anatomical structures and we assigned each ROI to a Brodmann area with the BioImage Suite software package (<http://www.bioimagesuite.org>, Lacadie et al., 2008).

Table 1 Coordinates (x, y, z) are in Talairach space (Talairach & Tournoux, 1988) of the areas studied here

Region	Left	Right	Broadmann area
Superior frontal gyrus (SFG)	$x \in [-35, -15]$	$x \in [30, 10]$	BA 9/BA 8
	$y \in [25, 55]$	$y \in [25, 55]$	
	$z \in [50, 35]$	$z \in [50, 35]$	
Middle frontal gyrus (MFG) dorsolateral prefrontal cortex (DLPFC)	$x \in [-50, -35]$	$x \in [45, 30]$	BA 46 (/BA 10), BA 8 / BA 9
	$y \in [25, 55]$	$y \in [25, 55]$	
	$z \in [30, 15]$	$z \in [20, 30]$	
Inferior frontal gyrus (IFG) ventrolateral prefrontal cortex (VLPFC)	$x \in [-60, -45]$	$x \in [60, 45]$	BA 44 (/BA 45)
	$y \in [15, 30]$	$y \in [15, 30]$	
	$z \in [15, 30]$	$z \in [15, 30]$	
Dorsal premotor (PMD) cortex	$x \in [-40, -15]$	$x \in [35, 10]$	BA 6
	$y \in [25, 55]$	$y \in [25, 55]$	
	$z \in [45, 60]$	$z \in [45, 60]$	

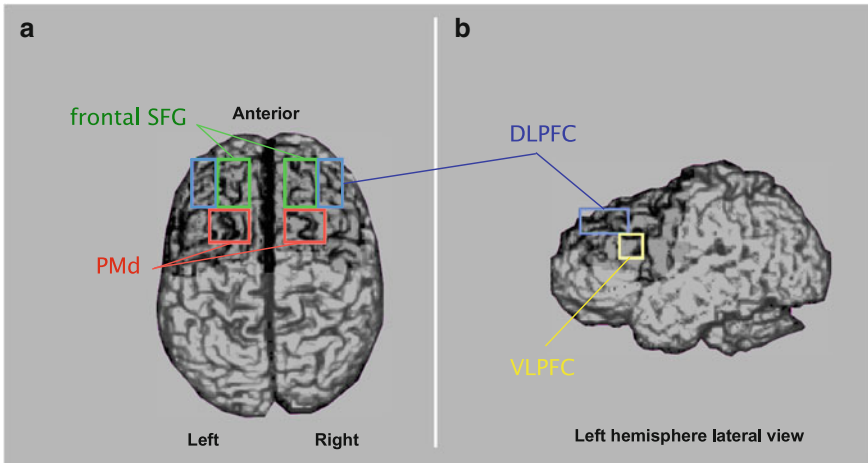


Fig. 2 Antero-posterior (a) and left hemisphere lateral (b) views of selected regions of interest (ROIs). The area in darker grey represents the brain region sampled by the recording montage. VLPFC: ventrolateral prefrontal cortex; DLPFC: dorsolateral prefrontal cortex; SFG: superior frontal gyrus; PMd: dorsal premotor cortex

3 Results

3.1 Grand Average ERPs

The sample size for the ERP analysis was $N = 7$ because one more subject (male) was excluded due to a technical problem that occurred during EEG data collection. The frequent and rare tones elicited similar negative ERP component between 120 and 150 ms (N1), followed by a small positive wave P2 (P180), along the midline sites, somewhat larger in the rare condition and towards frontal areas (Fig. 3a, B1). A second ERP peak negativity was mainly elicited in the rare tone condition at 230–260 ms post-stimulus (MMN/N2) at all three midline sites (Fig. 3a). We observed distinct topographic maps of electrical activity between the conditions during this time window (Fig. 3B2), but it was significantly different from the frequent tone ERP only on the frontal site ($p < 0.05$, Bonferroni-corrected for 64 electrodes). It is possible that such fronto-central N2 wave is a composite of N2a and N2b components, which overlap in time and scalp distribution.

Consistently with the literature, a significant difference between the two conditions ($p < 0.05$, Bonferroni-corrected for 64 electrodes) appeared for a large positive deflection elicited with a lag of approximately 300–400 ms (P300) after rare tones at all reported electrode sites. This positive wave included a fronto-central component P3a (Fig. 3B3) peaking between 280 and 330 ms and a second component P3b with

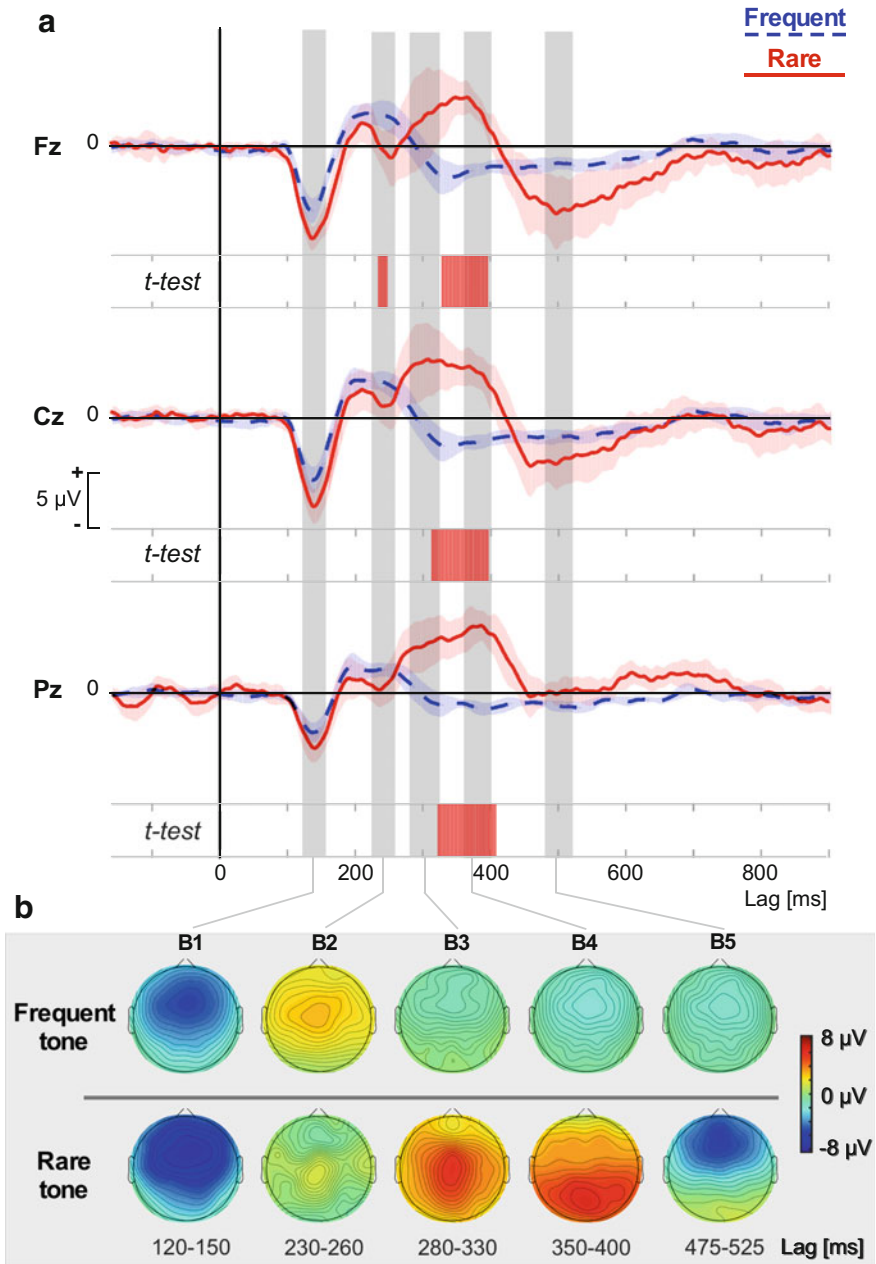


Fig. 3 **a** Grand average ERP waveforms (mean \pm 2 \times SEM) at electrode sites Fz, Cz and Pz ($N = 7$ participants). Each plot is followed by the result of a paired *t*-test between the frequent (dashed blue) and rare (red) tones (Bonferroni-corrected for 64 electrodes, in red when $p < 0.05$). **b** Topographic maps of scalp potential distribution at the main ERP components. **B1**: N1 at 120–150 ms post-stimulus; **B2**: MMN/N2 at 230–260 ms; **B3**: P3a at 280–330 ms; **B4**: P3b at 350–400 ms; **B5**: N500 (N400-like) at 475–525 ms

272 a posterior maximum (Fig. 3B4), peaking between 350 and 400 ms. A large frontal
273 negativity observed between 450 and 600 ms (N400-like/N500) was characterized
274 by maximal response over midline frontal electrodes (Fig. 3B5).

275 3.2 EROS

276 The data acquisition problem encountered during EEG recording of one participant
277 did not affect fNIRS, therefore the sample size for the EROS analysis was $N =$
278 8. The spatiotemporal profile of the optical signal response corresponded to the
279 topographical maps on group-level Z statistics of a 'differential EROS response',
280 which resulted from the contrasts conducted within the ROIs for each condition
281 separately relative to pre-stimulus baseline and for rare versus frequent tones, to the
282 three time points of the peak contrasts, i.e. at 40, 256, and 480 ms (Fig. 4).

283 Rare tones elicited less bilateral activation compared to frequent tones between
284 32 and 40 ms following the stimulus onset (Fig. 4A). In the left hemisphere, the
285 negative peak voxel activity was located in the Brodmann Area BA46 (DLPFC,
286 ROI in blue in Fig. 2, Talairach coordinates $x = -43$, $y = 27$) and did not reach
287 ($Z = -2.135$) the level of significance ($p = 0.05$) when averaging the voxels within
288 the ROI ($Z_{\text{crit}(0.05)} = -2.60$). The right negative peak voxel activity belonged to the
289 posterior part of BA8 ($x = 24$, $y = 27$) across superior frontal gyrus (ROI in green in
290 Fig. 2) and did not reach the ROI significance criterion ($Z = -2.169 > Z_{\text{crit}(0.05)} =$
291 -2.85).

292 At 256 ms post-stimulus, Fig. 4b shows the statistical maps resulting from dif-
293 ferential EROS responses and Fig. 5 shows also the responses in the rare and fre-
294 quent tone conditions, representing a complex pattern of activity co-occurring with
295 N2 component of the ERP. Between 240 and 272 ms in the rare tone condition,
296 we observed greater activation ($Z > 2$) in the ROI corresponding to the left PMd
297 (ROI in red in Fig. 2, $x = -21$, $y = 12$, BA6) with a peak voxel activity at 256 ms
298 ($Z = 2.263 < Z_{\text{crit}(0.05)} = 2.67$). Between 240 and 264 ms, we observed a reduced
299 differential EROS response in the right SFG (BA8, $x = 24$, $y = 29$) with a peak
300 voxel activity at 256 ms ($Z = -2.368 > Z_{\text{crit}(0.05)} = -2.89$). Those two effects were
301 very close to their ROI criterion of significance at $p = 0.05$.

302 Broca's area (VLPFC, ROI in yellow in Fig. 2, $y = 22$, $z = 22$), correspond-
303 ing to BA44 contained and limited by pars opercularis of the left inferior frontal
304 gyrus, was characterized by a greater activation in the rare tone condition in the
305 interval 248–264 ms with a significant peak voxel activity at 264 ms ($Z = 2.234$
306 $> Z_{\text{crit}(0.05)} = 2.20$). This ROI was activated almost exclusively during the rare
307 tone condition, as emphasized by the significant contrast (maximum at 272 ms,
308 $Z = 2.245 > Z_{\text{crit}(0.05)} = 2.19$) of this condition with the baseline between 248 and
309 280 ms (Fig. 5b, sagittal projection). In the left hemisphere, it is interesting to notice
310 also an activation at the level of the auditory cortex in the postcentral gyrus (BA 43)
311 only after frequent tones (Fig. 5c). This activation fell below a significant contrast
312 ($Z < 2$) and was not visible in the differential EROS response (Fig. 5a).

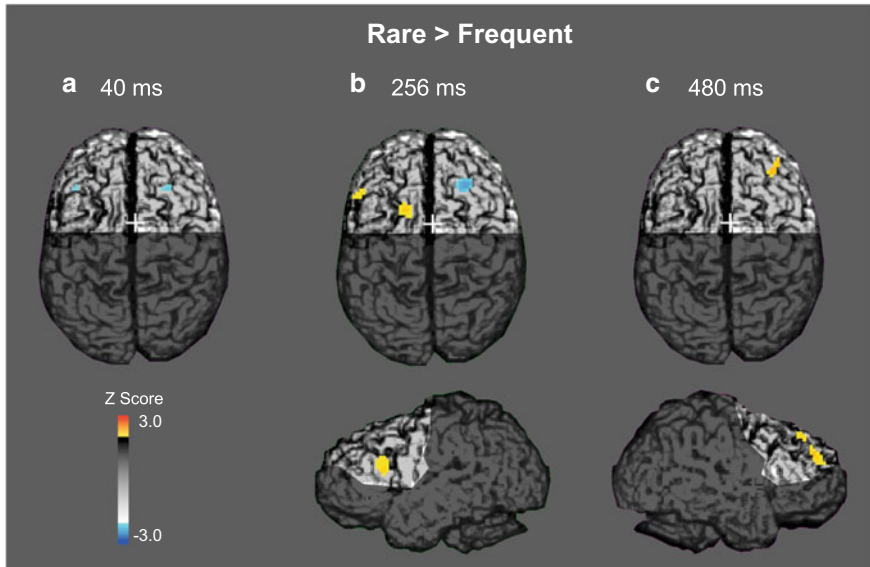


Fig. 4 Spatial maps based on group-level ($N = 8$) Z statistics for the EROS data contrasting rare versus frequent tones in the passive auditory oddball task relative to the pre-stimulus baseline. The area in light grey represents the brain region sampled by the recording montage. **a** Projection of EROS data to the axial surface at 40 ms after stimulus onset. The differential EROS response shows that superior frontal gyrus was activated after frequent tones by the dorsal spatial (“where”) processing stream, BA46 in the left hemisphere and BA8 in the right hemisphere. **b** Spatial maps of the EROS data projected to the axial (top) and left sagittal (bottom) surfaces of significant ROIs at 256 ms after stimulus onset, co-occurring with N2b ERP wave. Notice the complex pattern of response, see Fig. 5 for more details. **c** Projection to the axial (top) and right sagittal (bottom) surfaces of significant ROIs at 480 ms after stimulus onset, co-occurring with N500 (N400-like) ERP wave. In the right hemisphere, notice the strong activation of DLPFC after rare tones at the level of BA9 (axial projection) and BA46 (sagittal projection)

313 In the right middle frontal gyrus (Fig. 4C), at the level of BA9 of DLPFC (Talairach
 314 coordinates $x = 32$, $y = 39$), a greater activation was observed between 464 and
 315 520 ms in the rare tone condition with a peak voxel activity at 488 ms ($Z = 2.361 <$
 316 $Z_{\text{crit}(0.05)} = 2.97$). This activation co-occurred with the N500 (N400-like) ERP wave.
 317 A more anterior part of DLPFC, corresponding to BA46 (see the right hemisphere
 318 sagittal view of Fig. 4c), was also activated by the differential EROS response during
 319 this interval, but it was located outside the predefined ROIs.

320 4 Discussion

321 We report results on the neural dynamics of frontal cortex response to a passive
 322 auditory oddball task studied by simultaneous recording of fast optical signals with
 323 high temporal resolution (EROS) and ERPs. To the best of our knowledge, no other

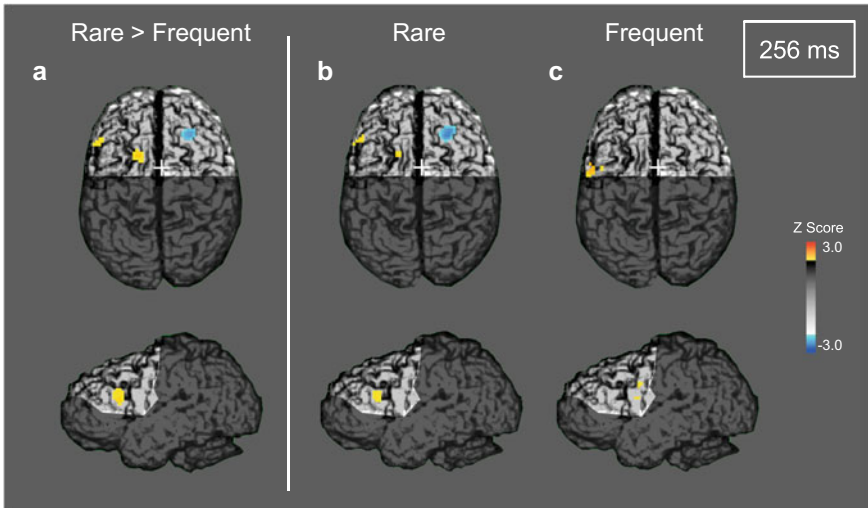


Fig. 5 Spatial maps based on group-level ($N = 8$) Z statistics for the EROS data at 256 ms after tone onset, co-occurring with N2b ERP wave, projected to the axial (top) and left sagittal (bottom) surfaces. **a** Response contrasting rare versus frequent tones compared to pre-stimulus baseline, same as Fig. 4b. **b** Response to rare tones separately contrasted with pre-stimulus baseline. Notice the same ROIs visible in panel (a), although with a different significant voxel density. **c** Response to frequent tones contrasted with pre-stimulus baseline. Notice a small activation in the postcentral gyrus, at the border of the area under investigation

324 study has yet combined EROS with a similar temporal resolution (i.e. 8 ms sampling
 325 time) with a 64-channel EEG system in an auditory oddball task. Electrophysiological
 326 recordings revealed all the ERP components (N1, P2, N2, P3) well described in the
 327 literature (Alexander et al., 1994; Michalewski et al., 1986; Näätänen, 1990). We
 328 observed also several commonalities and some differences regarding the brain areas
 329 and the response timing with the few previous studies reporting EROS analyses in
 330 auditory and visual oddball tasks (Low et al., 2006; Proulx et al., 2018; Tse & Penney,
 331 2008; Tse et al., 2006, 2013). Despite controversial observation about the significance
 332 of fast optical signals measured by fNIRS (Steinbrink et al., 2005; Syré et al., 2003),
 333 the co-occurrence of optical signals and ERP waves found here confirms that such
 334 a methodological approach carries the potential for investigating neurodynamics of
 335 cognitive activity in a wide range of tasks (Gratton et al., 2018). However, there
 336 are several limitations that should be acknowledged in our results. First, this study
 337 may be considered somewhat preliminary because of the small sample size ($N = 7$
 338 for ERP and $N = 8$ for EROS analyses), although the statistical analyses showed
 339 suitable effects. Additional data are being collected and a final report with a larger
 340 sample will be soon completed. Second, fast optical signals suffer from a low signal-
 341 to-noise ratio and the response signal is limited to a few centimeters below the scalp
 342 (Gratton & Fabiani, 2010). It is important to underline that complementary studies
 343 using different and independent measures of brain activity are necessary to gain

344 further insights of the spatiotemporal patterns of brain dynamics while performing
345 behavioral tasks.

346 After the stimulus onset, the earliest response observed in this study is an optical
347 signal in the differential EROS response, appeared as early as between 32 and 40 ms
348 post-stimulus showing a bilateral activation that is larger for frequent than rare stim-
349 uli, thus suggesting a short latency input from the auditory system. The localization
350 of the signal at the level of BA46 of DLPFC in the left hemisphere and at the level
351 of BA8 of the superior frontal gyrus in the right hemisphere suggests that the input
352 is not from the sensory ascending subcortical pathway. The DLPFC is the end point
353 for the dorsal stream that transmits spatial (“where”) information (Ahveninen et al.,
354 2006; Plakke & Romanski, 2016).

355 The next evoked activity response was an ERP component with a negative peak
356 observed along the midline, mainly fronto-central sites, between 120 and 150 ms
357 post-stimulus followed by a smaller positive wave. The profile and the latency of this
358 wave was similar after frequent and rare tones, although the amplitude after rare tones
359 tended to be larger. The latency and localization of this peak is in agreement with
360 the N1/P2 (N100-P200) complex reported for the auditory oddball task with strong
361 generators in the auditory areas of the STG and with association with a stimulus-
362 driven attention-trigger mechanism (Näätänen & Picton, 1987; Rinne et al., 1999).
363 In previous imaging studies coupled with EEG, the N100 component during auditory
364 tasks co-occurred also with a signal in the anterior cingulate cortex (ACC) (Esposito
365 et al., 2009; Walz et al., 2013). At this latency, we could not observe any significant
366 optical response in our ROIs of the prefrontal cortex. This is likely due to the fact
367 that our fNIRS montage was not designed to record neither from the auditory cortex
368 nor from ACC.

369 The typical event-related response to the stimulus presentation observed in the
370 auditory oddball task is the N2/P3 (P300) wave complex (Alexander et al., 1994;
371 Fabiani & Friedman, 1995; Näätänen & Picton, 1987; Squires et al., 1975). This
372 wave is characterized by several components, which may overlap in time and scalp
373 distribution. We observed a fronto-central N2b-P3a component (Fig. 3B2 and B3)
374 between 230 and 330 ms post-stimulus, followed by a P3b component with a parietal
375 maximum (Fig. 3B4), peaking between 350 and 400 ms. Source locations determined
376 from fMRI showed that the ACC was the principal generator of N2b-P3a ERP wave
377 following dipole modeling of ERPs (Crottaz-Herbette & Menon, 2006). We observed
378 fast optical signals correlated with the timing of this wave, but their latency was
379 different (up to approximately 100 ms later) than the lag reported from other oddball-
380 related EROS analyses (Low et al., 2006, 2009; Proulx et al., 2018; Tse et al., 2006,
381 2013; Tse & Penney, 2008). Differences in the protocol of our passive oddball task
382 with respect to previous studies might explain differences in the temporal profile
383 of the response. The current occurrence probability of rare (i.e., deviant) stimuli
384 was $p = 8\%$ compared to $p = 20\%$ (Low et al., 2006, 2009; Proulx et al., 2018),
385 which could suggest that in our protocol rare tones were likely to be much more
386 unattended. The duration of our tones was 500 ms, that was much longer than usual
387 stimuli duration in oddball studies, i.e. 70–100 ms (Ruusuvirta et al., 2007; Tse &
388 Penney, 2008; Tse et al., 2006, 2013), and longer than 400 ms used in similar EROS

389 settings (Baniqued et al., 2013; Low et al., 2006, 2009). Moreover, we 1500 Hz
390 instead 500 Hz for the rare tone frequency pip and 60 dB SPL instead of 70 dB
391 SPL for the loudness (Low et al., 2006, 2009; Proulx et al., 2018). Hence, our
392 protocol might have triggered a different dynamics or slightly different processes
393 that we observed in our EROS analysis. Filtering parameters are very important for
394 the detection of fast optical signals with a low signal-to-noise ratio (Maclin et al.,
395 2003). In this study EROS was bandpass filtered in the range 0.1–10 Hz, compared
396 to 0–5 Hz (Low et al., 2006, 2009), 0.5–10 Hz (Baniqued et al., 2013), 1–10/12 Hz
397 (Tse & Penney, 2008; Tse et al., 2006, 2013), and 2–20 Hz (Proulx et al., 2018) of
398 the other studies.

399 The differential EROS response occurring at the same time of the N2/P3 ERP
400 showed an activation in the inferior frontal gyrus at the level of left PMd (BA6) for
401 the rare tones. Both action control and action observation require premotor functions
402 and left PMd participates to mapping external action parameters onto the appropriate
403 motor repertoire (Moisa et al., 2012; Stadler et al., 2012). In addition to the premotor
404 functions, our finding supports the hypothesis that the activation of the left PMd
405 may reflect encoding of the semantic features of actions (i.e., cognitive aspects of
406 the sensorimotor sequences associated with the detection of deviant stimuli) (Press
407 et al., 2012). Around at the same time, a pattern of activation opposite to this one
408 for PMd was observed for EROS in the superior frontal gyrus at the level of BA8,
409 near the border of BA46 in the DLPFC. This area was slightly activated by frequent
410 tones, but it was strongly deactivated by rare tones compared to baseline activity.
411 This signal was not observed by Low et al. (2006), but in their study rare tones were
412 less unattended (20% of the total number of stimuli vs. 8% in our protocol). BA46 is
413 mostly related with the executive control of language production (Ardila et al., 2016)
414 and we suggest that the source of the observed signal was rather BA8. This area of
415 right DLPFC is involved in pitch and memory processing of the auditory stimulus
416 (Kumar et al., 2015; Schaal et al., 2017). Hence, our results might suggest that in the
417 passive oddball task this part of BA8 would be more active when a retrieval attempt
418 of the frequent tone succeeded than when it failed.

419 We observed an optical signal in the left VLPFC (BA44, Broca's area) occurring
420 with N2 ERP component, in agreement with previous studies (Linden et al., 1999;
421 Medvedev et al., 2010; Tse et al., 2006). The activation in BA44 was strong after
422 rare tones and occurred about at the same time of a lesser activated area in the left
423 postcentral gyrus (BA43) after frequent tones. The anterior ventral stream that brings
424 information about the stimuli's characteristics (i.e., processing an object "what"
425 information) projects to VLPFC (Ahveninen et al., 2006; Plakke & Romanski, 2016).
426 Broca's area (BA44 in the left VLPFC) is involved in semantic tasks, in the motor
427 aspect of speech, and in music perception (Bezgin et al., 2014; Flinker et al., 2015;
428 Levitin & Tirovolas, 2009). The activation of BA43 and surrounding areas in STG
429 was reported for abstract auditory representations and mental imagery of speech
430 (Chiang et al., 2013; Tian et al., 2016). The differential spatial pattern of response
431 observed in our results, between BA44 and BA43, might suggest that the oddball
432 task could engage inhibitory processes triggered by deviant stimuli, as suggested in
433 the literature in association with theta band oscillations (Harper et al., 2014; Jonides

434 et al., 1998; Proulx et al., 2018). We did not analyze here these oscillations, but this
435 is certainly an interesting analysis to be developed in our extended experiment and
436 future studies.

437 Previous studies have shown ERP negative waves at a latency between 300 and 500
438 ms post-stimulus elicited in target detection and oddball tasks (Codispoti et al., 2006;
439 Kiehl et al., 2006; Low et al., 2006; Stevens et al., 2005), which was observed in our
440 results as a large N500 (N400-like) wave. Our ERP analysis showed that N500 was
441 almost exclusively elicited by rare tones and its amplitude was much larger for Fz, in
442 agreement with the frontal and right hemisphere topographical distribution reported
443 in those previous studies. The N400-like component has been usually reported with
444 a spatial distribution over centro-parietal or centro-posterior sites in lexical decision
445 tasks and in relation to predictability of stimuli and in the inferior frontal regions,
446 if the effect reflected integration difficulty (Kutas & Hillyard, 1984; Kutas & Fed-
447 ermeier, 2000; Lau et al., 2008; Rossi et al., 2013). Our EROS analysis showed an
448 activation at the level of DLPFC, more specifically in the right hemisphere for two
449 close regions across the Brodmann areas BA9 and BA46. Neuroimaging analysis by
450 fMRI reported that the DLPFC corresponding to the areas BA9/BA46 in the right
451 middle frontal gyrus was involved in maintaining integrated information (Collette
452 et al., 2005; Prabhakaran et al., 2000), associated with the acquisition of abstract
453 rules (Monte-Ordoño & Toro, 2017; Sun et al., 2012) and accompanying conscious
454 experience of abstract auditory percepts (Brancucci et al., 2016).

455 5 Conclusion

456 The data of the current study demonstrate that cognitive neural dynamics or pre-
457 frontal cortical activity during a passive auditory oddball task can be studied by a
458 non-invasive fast optical imaging technique (EROS) with co-localized EEG mea-
459 surements. We identified significant co-occurrences of EROS and ERP responses to
460 rare tones. By combining high spatial and temporal resolution we observed that left
461 and right pre-frontal structures were differentially affected. The left dorsal premo-
462 tor cortex and Broca's area in the left VLPFC were activated by rare tones during
463 the mismatch negativity and N2 ERP components, whereas frequent tones activated
464 a small area in the right superior frontal gyrus involved in memory processing of
465 the auditory stimulus. Moreover, our results showed a significant N500 (N400-like)
466 wave associated with the activity of DLPFC after rare tones, likely related with the
467 maintenance of integrated information.

468 **Acknowledgements** We acknowledge the support by the Swiss National Science Foundation, grant
469 no. POLAPI_178329 for MEJ and grant no. IZSEZO_183401 for RK.

References

- 470
- 471 Ahveninen, J., Jääskeläinen, I. P., Raij, T., Bonmassar, G., Devore, S., Hämäläinen, M., et al. (2006).
 472 Task-modulated "what" and "where" pathways in human auditory cortex. *Proc Natl Acad Sci U*
 473 *S A*, *103*(39), 14608–13.
- 474 Alexander, J. E., Polich, J., Bloom, F. E., Bauer, L. O., Kuperman, S., Rohrbaugh, J., et al. (1994).
 475 P300 from an auditory oddball task: inter-laboratory consistency. *Int J Psychophysiol*, *17*(1),
 476 35–46.
- 477 Apelbaum, J., Silva, E. E., Frick, O., & Segundo, J. P. (1960). Specificity and biasing of arousal
 478 reaction habituation. *Electroencephalogr Clin Neurophysiol*, *12*, 829–840.
- 479 Ardila, A., Bernal, B., & Rosselli, M. (2016). How Localized are Language Brain Areas? A Review
 480 of Brodmann Areas Involvement in Oral Language. *Arch Clin Neuropsychol*, *31*(1), 112–22.
- 481 Baniqued, P. L., Low, K. A., Fabiani, M., & Gratton, G. (2013). Frontoparietal traffic signals: a fast
 482 optical imaging study of preparatory dynamics in response mode switching. *J Cogn Neurosci*,
 483 *25*(6), 887–902.
- 484 Bezgin, G., Rybacki, K., van Opstal, A. J., Bakker, R., Shen, K., Vakorin, V. A., et al. (2014).
 485 Auditory-prefrontal axonal connectivity in the macaque cortex: quantitative assessment of pro-
 486 cessing streams. *Brain Lang*, *135*, 73–84.
- 487 Blumstein, D. T. (2016). Habituation and sensitization: new thoughts about old ideas. *Anim Behav*,
 488 *120*, 255–262.
- 489 Brancucci, A., Lugli, V., Perrucci, M. G., Del Gratta, C., & Tommasi, L. (2016). A frontal but not
 490 parietal neural correlate of auditory consciousness. *Brain Struct Funct*, *221*(1), 463–72.
- 491 Chance, B., Zhuang, Z., UnAh, C., Alter, C., & Lipton, L. (1993). Cognition-activated low-frequency
 492 modulation of light absorption in human brain. *Proc Natl Acad Sci U S A*, *90*(8), 3770–3774.
- 493 Chiang, T.-C., Liang, K.-C., Chen, J.-H., Hsieh, C.-H., & Huang, Y.-A. (2013). Brain deactivation
 494 in the outperformance in bimodal tasks: an fMRI study. *PLoS One*, *8*(10), e77408.
- 495 Codispoti, M., Ferrari, V., Junghöfer, M., & Schupp, H. T. (2006). The categorization of natural
 496 scenes: brain attention networks revealed by dense sensor ERPs. *Neuroimage*, *32*(2), 583–91.
- 497 Collette, F., Olivier, L., Van der Linden, M., Laureys, S., Delfiore, G., Luxen, A., et al. (2005).
 498 Involvement of both prefrontal and inferior parietal cortex in dual-task performance. *Brain Res*
 499 *Cogn Brain Res*, *24*(2), 237–51.
- 500 Crottaz-Herbette, S., & Menon, V. (2006). Where and when the anterior cingulate cortex modulates
 501 attentional response: combined fMRI and ERP evidence. *J Cogn Neurosci*, *18*(5), 766–80.
- 502 Delorme, A., & Makeig, S. (2004). EEGLAB: an open source toolbox for analysis of single-trial
 503 EEG dynamics including independent component analysis. *J Neurosci Methods*, *134*(1), 9–21.
- 504 Delpy, D. T., & Cope, M. (1997). Quantification in tissue near-infrared spectroscopy. *Philos Trans*
 505 *R Soc Lond B Biol Sci*, *352*(1354), 649–659.
- 506 Eriksson, J. L., & Villa, A. E. P. (2005). Event-related potentials in an auditory oddball situation in
 507 the rat. *BioSystems*, *79*(1–3), 207–212.
- 508 Esposito, F., Mulert, C., & Goebel, R. (2009). Combined distributed source and single-trial EEG-
 509 fMRI modeling: application to effortful decision making processes. *Neuroimage*, *47*(1), 112–21.
- 510 Fabiani, M., & Friedman, D. (1995). Changes in brain activity patterns in aging: the novelty oddball.
 511 *Psychophysiology*, *32*(6), 579–94.
- 512 Flinker, A., Korzeniewska, A., Shestyuk, A. Y., Franaszczuk, P. J., Dronkers, N. F., Knight, R. T.,
 513 et al. (2015). Redefining the role of Broca's area in speech. *Proc Natl Acad Sci U S A*, *112*(9),
 514 2871–5.
- 515 Gaillard, A. W. (1976). Effects of warning-signal modality on the contingent negative variation
 516 (CNV). *Biol Psychol*, *4*(2), 139–54.
- 517 Goodin, D. S., Squires, K. C., Henderson, B. H., & Starr, A. (1978). An early event-related cortical
 518 potential. *Psychophysiology*, *15*(4), 360–365.
- 519 Gratton, E., Fantini, S., Franceschini, M. A., Gratton, G., & Fabiani, M. (1997). Measurements
 520 of scattering and absorption changes in muscle and brain. *Philos Trans R Soc Lond B Biol Sci*,
 521 *352*(1354), 727–35.



- 522 Gratton, G. (2000). "Opt-cont" and "Opt-3D": A software suite for the analysis and 3D reconstruction
523 of the event-related optical signal (EROS). *Psychophysiology*, 37, S44.
- 524 Gratton, G., Brumback, C. R., Gordon, B. A., Pearson, M. A., Low, K. A., & Fabiani, M. (2006).
525 Effects of measurement method, wavelength, and source-detector distance on the fast optical
526 signal. *NeuroImage*, 32(4), 1576–1590.
- 527 Gratton, G., Cooper, P., Fabiani, M., Carter, C. S., & Karayanidis, F. (2018). Dynamics of cognitive
528 control: Theoretical bases, paradigms, and a view for the future. *Psychophysiology*, 55(3), e13016.
- 529 Gratton, G., & Corballis, P. M. (1995). Removing the heart from the brain: compensation for the
530 pulse artifact in the photon migration signal. *Psychophysiology*, 32(3), 292–299.
- 531 Gratton, G., Corballis, P. M., Cho, E., Fabiani, M., & Hood, D. C. (1995). Shades of gray matter: non-
532 invasive optical images of human brain responses during visual stimulation. *Psychophysiology*,
533 32(5), 505–509.
- 534 Gratton, G., & Fabiani, M. (1998). Dynamic brain imaging: Event-related optical signal (EROS)
535 measures of the time course and localization of cognitive-related activity. *Psychon Bull Rev*, 5(4),
536 535–563.
- 537 Gratton, G., & Fabiani, M. (2001). Shedding light on brain function: the event-related optical signal.
538 *Trends Cogn Sci*, 5(8), 357–363.
- 539 Gratton, G., & Fabiani, M. (2010). Fast optical imaging of human brain function. *Front Hum*
540 *Neurosci*, 4, e00052.
- 541 Harper, J., Malone, S. M., & Bernat, E. M. (2014). Theta and delta band activity explain N2 and P3
542 ERP component activity in a go/no-go task. *Clin Neurophysiol*, 125(1), 124–132.
- 543 Horowitz, S. G., Skudlarski, P., & Gore, J. C. (2002). Correlations and dissociations between BOLD
544 signal and P300 amplitude in an auditory oddball task: a parametric approach to combining fMRI
545 and ERP. *Magn Reson Imaging*, 20(4), 319–25.
- 546 Jausovec, N., & Jausovec, K. (2009). Do women see things differently than men do? *Neuroimage*,
547 45(1), 198–207.
- 548 Jeong, E., Ryu, H., Jo, G., & Kim, J. (2018). Cognitive Load Changes during Music Listening and
549 its Implication in Earcon Design in Public Environments: An fNIRS Study. *Int J Environ Res*
550 *Public Health*, 15(10), e2075.
- 551 Jonides, J., Smith, E. E., Marshuetz, C., Koeppe, R. A., & Reuter-Lorenz, P. A. (1998). Inhibition in
552 verbal working memory revealed by brain activation. *Proc Natl Acad Sci U S A*, 95(14), 8410–3.
- 553 Kennan, R. P., Horovitz, S. G., Maki, A., Yamashita, Y., Koizumi, H., & Gore, J. C. (2002). Simul-
554 taneous recording of event-related auditory oddball response using transcranial near infrared
555 optical topography and surface EEG. *Neuroimage*, 16(3), 587–592.
- 556 Kiehl, K. A., Bates, A. T., Laurens, K. R., Hare, R. D., & Liddle, P. F. (2006). Brain potentials
557 implicate temporal lobe abnormalities in criminal psychopaths. *J Abnorm Psychol*, 115(3), 443–
558 53.
- 559 Kubota, M., Inouchi, M., Dan, I., Tsuzuki, D., Ishikawa, A., & Scovel, T. (2008). Fast (100–175 ms)
560 components elicited bilaterally by language production as measured by three-wavelength optical
561 imaging. *Brain Res*, 1226, 124–33.
- 562 Kumar, U., Guleria, A., & Khetrapal, C. L. (2015). Neuro-cognitive aspects of "OM" sound/syllable
563 perception: A functional neuroimaging study. *Cogn Emot*, 29(3), 432–41.
- 564 Kutas, M., & Federmeier, K. D. (2000). Electrophysiology reveals semantic memory use in language
565 comprehension. *Trends Cogn Sci*, 4(12), 463–470.
- 566 Kutas, M., & Hillyard, S. A. (1984). Brain potentials during reading reflect word expectancy and
567 semantic association. *Nature*, 307(5947), 161–163.
- 568 Lacadie, C. M., Fulbright, R. K., Rajeevan, N., Constable, R. T., & Papademetris, X. (2008). More
569 accurate Talairach coordinates for neuroimaging using non-linear registration. *Neuroimage*, 42(2),
570 717–25.
- 571 Lau, E. F., Phillips, C., & Poeppel, D. (2008). A cortical network for semantics: (de)constructing
572 the N400. *Nat Rev Neurosci*, 9(12), 920–33.
- 573 Lee, J., & Kim, S. J. (2010). Spectrum measurement of fast optical signal of neural activity in brain
574 tissue and its theoretical origin. *Neuroimage*, 51(2), 713–22.

- 575 Levitin, D. J., & Tirovolas, A. K. (2009). Current Advances in the Cognitive Neuroscience of Music.
576 *Ann N Y Acad Sci*, 1156(1), 211–231.
- 577 Linden, D. E., Prvulovic, D., Formisano, E., Völlinger, M., Zanella, F. E., Goebel, R., et al. (1999).
578 The functional neuroanatomy of target detection: an fMRI study of visual and auditory oddball
579 tasks. *Cereb Cortex*, 9(8), 815–23.
- 580 Liu, X., Iwanaga, K., & Koda, S. (2011). Circulatory and central nervous system responses to
581 different types of mental stress. *Ind Health*, 49(3), 265–73.
- 582 Low, K. A., Leaver, E., Kramer, A. F., Fabiani, M., & Gratton, G. (2006). Fast optical imaging of
583 frontal cortex during active and passive oddball tasks. *Psychophysiology*, 43(2), 127–36.
- 584 Low, K. A., Leaver, E. E., Kramer, A. F., Fabiani, M., & Gratton, G. (2009). Share or compete? Load-
585 dependent recruitment of prefrontal cortex during dual-task performance. *Psychophysiology*,
586 46(5), 1069–79.
- 587 Maclin, E. L., Gratton, G., & Fabiani, M. (2003). Optimum filtering for EROS measurements.
588 *Psychophysiology*, 40(4), 542–7.
- 589 Mangalathu-Arumana, J., Beardsley, S. A., & Liebenthal, E. (2012). Within-subject joint indepen-
590 dent component analysis of simultaneous fMRI/ERP in an auditory oddball paradigm. *Neuroim-
591 age*, 60(4), 2247–2257.
- 592 McCarthy, G., Luby, M., Gore, J., & Goldman-Rakic, P. (1997). Infrequent events transiently activate
593 human prefrontal and parietal cortex as measured by functional mri. *J Neurophysiol*, 77(3), 1630–
594 1634.
- 595 Medvedev, A. V., Kainerstorfer, J., Borisov, S. V., Barbour, R. L., & VanMeter, J. (2008). Event-
596 related fast optical signal in a rapid object recognition task: improving detection by the indepen-
597 dent component analysis. *Brain Res*, 1236, 145–58.
- 598 Medvedev, A. V., Kainerstorfer, J. M., Borisov, S. V., Gandjbakhche, A. H., & Vanmeter, J. (2010).
599 "seeing" electroencephalogram through the skull: imaging prefrontal cortex with fast optical
600 signal. *J Biomed Opt*, 15(6), 061702.
- 601 Menon, V., Ford, J. M., Lim, K. O., Glover, G. H., & Pfefferbaum, A. (1997). Combined event-
602 related fMRI and EEG evidence for temporal-parietal cortex activation during target detection.
603 *Neuroreport*, 8(14), 3029–3037.
- 604 Michalewski, H. J., Prasher, D. K., & Starr, A. (1986). Latency variability and temporal inter-
605 relationships of the auditory event-related potentials (N1, P2, N2, and P3) in normal subjects.
606 *Electroencephalogr Clin Neurophysiol*, 65(1), 59–71.
- 607 Moisa, M., Siebner, H. R., Pohmann, R., & Thielscher, A. (2012). Uncovering a context-specific
608 connective fingerprint of human dorsal premotor cortex. *J Neurosci*, 32(21), 7244–52.
- 609 Molnár, M. (1994). On the origin of the P3 event-related potential component. *Int J Psychophysiol*,
610 17(2), 129–44.
- 611 Monte-Ordoño, J., & Toro, J. M. (2017). Different ERP profiles for learning rules over consonants
612 and vowels. *Neuropsychologia*, 97, 104–111.
- 613 Näätänen, R. (1990). The role of attention in auditory information processing as revealed by event-
614 related potentials and other brain measures of cognitive function. *Behav Brain Sci*, 13, 201–288.
- 615 Näätänen, R., & Picton, T. (1987). The N1 wave of the human electric and magnetic response to
616 sound: a review and an analysis of the component structure. *Psychophysiology*, 24(4), 375–425.
- 617 Nunez, P. (1995). *Neocortical Dynamics and Human EEG Rhythms*. Oxford University Press, New
618 York, NY., xii, 708 pages.
- 619 Okada, E., Firbank, M., Schweiger, M., Arridge, S. R., Cope, M., & Delpy, D. T. (1997). Theoretical
620 and experimental investigation of near-infrared light propagation in a model of the adult head.
621 *Appl Opt*, 36(1), 21–31.
- 622 Opitz, B., Mecklinger, A., Von Cramon, D. Y., & Kruggel, F. (1999). Combining electrophysiologi-
623 cal and hemodynamic measures of the auditory oddball. *Psychophysiology*, 36(1), 142–7.
- 624 Plakke, B., & Romanski, L. M. (2016). Neural circuits in auditory and audiovisual memory. *Brain
625 Res*, 1640, 278–88.
- 626 Polich, J. (2007). Updating P300: an integrative theory of P3a and P3b. *Clin Neurophysiol*, 118(10),
627 2128–2148.



- 628 Prabhakaran, V., Narayanan, K., Zhao, Z., & Gabrieli, J. D. (2000). Integration of diverse information
629 in working memory within the frontal lobe. *Nat Neurosci*, 3(1), 85–90.
- 630 Press, C., Weiskopf, N., & Kilner, J. M. (2012). Dissociable roles of human inferior frontal gyrus
631 during action execution and observation. *Neuroimage*, 60(3), 1671–7.
- 632 Proulx, N., Samadani, A.-A., & Chau, T. (2018). Quantifying fast optical signal and event-related
633 potential relationships during a visual oddball task. *Neuroimage*, 178, 119–128.
- 634 Rinne, T., Gratton, G., Fabiani, M., Cowan, N., Maclin, E., Stinard, A., et al. (1999). Scalp-recorded
635 optical signals make sound processing in the auditory cortex visible? *Neuroimage*, 10(5), 620–4.
- 636 Rossi, S., Hartmüller, T., Vignotto, M., & Obrig, H. (2013). Electrophysiological evidence for
637 modulation of lexical processing after repetitive exposure to foreign phonotactic rules. *Brain*
638 *Lang*, 127(3), 404–14.
- 639 Ruusuvirta, T., Huotilainen, M., & Näätänen, R. (2007). Preperceptual human number sense for
640 sequential sounds, as revealed by mismatch negativity brain response? *Cereb Cortex*, 17(12),
641 2777–9.
- 642 Ruusuvirta, T., Korhonen, T., Arikoski, J., & Kivirikko, K. (1996). ERPs to pitch changes: a result
643 of reduced responses to standard tones in rabbits. *Neuroreport*, 7(2), 413–416.
- 644 Schaal, N. K., Kretschmer, M., Keitel, A., Krause, V., Pfeifer, J., & Pollok, B. (2017). The Signifi-
645 cance of the Right Dorsolateral Prefrontal Cortex for Pitch Memory in Non-musicians Depends
646 on Baseline Pitch Memory Abilities. *Front Neurosci*, 11, e00677.
- 647 Scholkmann, F., Kleiser, S., Metz, A. J., Zimmermann, R., Mata Pavia, J., Wolf, U., et al. (2014). A
648 review on continuous wave functional near-infrared spectroscopy and imaging instrumentation
649 and methodology. *Neuroimage*, 85, 6–27.
- 650 Squires, N. K., Squires, K. C., & Hillyard, S. A. (1975). Two varieties of long-latency positive
651 waves evoked by unpredictable auditory stimuli in man. *Electroencephalogr Clin Neurophysiol*,
652 38(4), 387–401.
- 653 Stadler, W., Ott, D. V. M., Springer, A., Schubotz, R. I., Schütz-Bosbach, S., & Prinz, W. (2012).
654 Repetitive TMS suggests a role of the human dorsal premotor cortex in action prediction. *Front*
655 *Hum Neurosci*, 6, e00020.
- 656 Steinbrink, J., Kempf, F. C. D., Villringer, A., & Obrig, H. (2005). The fast optical signal-robust or
657 elusive when non-invasively measured in the human adult? *Neuroimage*, 26(4), 996–1008.
- 658 Steinbrink, J., Kohl, M., Obrig, H., Curio, G., Syré, F., Thomas, F., et al. (2000). Somatosensory
659 evoked fast optical intensity changes detected non-invasively in the adult human head. *Neurosci*
660 *Lett*, 291(2), 105–8.
- 661 Stevens, M. C., Calhoun, V. D., & Kiehl, K. A. (2005). Hemispheric differences in hemodynamics
662 elicited by auditory oddball stimuli. *Neuroimage*, 26(3), 782–792.
- 663 Strait, M., & Scheutz, M. (2014). What we can and cannot (yet) do with functional near infrared
664 spectroscopy. *Front Neurosci*, 8, e00117.
- 665 Sun, F., Hoshi-Shiba, R., Abla, D., & Okanoya, K. (2012). Neural correlates of abstract rule learning:
666 an event-related potential study. *Neuropsychologia*, 50(11), 2617–24.
- 667 Syré, F., Obrig, H., Steinbrink, J., Kohl, M., Wenzel, R., & Villringer, A. (2003). Are VEP correlated
668 fast optical signals detectable in the human adult by non-invasive nearinfrared spectroscopy
669 (NIRS)? *Adv Exp Med Biol*, 530, 421–31.
- 670 Talairach, J. and Tournoux, P. (1988). *Co-Planar Stereotaxic Atlas of the Human Brain. 3-*
671 *Dimensional Proportional System: An Approach to Cerebral Imaging*. Georg Thieme Verlag.
- 672 Thompson, R. F. (2009). Habituation: a history. *Neurobiol Learn Mem*, 92(2), 127–134.
- 673 Tian, X., Zarate, J. M., & Poeppel, D. (2016). Mental imagery of speech implicates two mechanisms
674 of perceptual reactivation. *Cortex*, 77, 1–12.
- 675 Torricelli, A., Contini, D., Pifferi, A., Caffini, M., Re, R., Zucchelli, L., et al. (2014). Time domain
676 functional nirs imaging for human brain mapping. *Neuroimage*, 85, 28–50.
- 677 Tse, C.-Y., & Penney, T. B. (2008). On the functional role of temporal and frontal cortex activation
678 in passive detection of auditory deviance. *Neuroimage*, 41(4), 1462–70.
- 679 Tse, C.-Y., Rinne, T., Ng, K. K., & Penney, T. B. (2013). The functional role of the frontal cortex
680 in pre-attentive auditory change detection. *Neuroimage*, 83, 870–879.

- 681 Tse, C.-Y., Tien, K.-R., & Penney, T. B. (2006). Event-related optical imaging reveals the tempo-
682 ral dynamics of right temporal and frontal cortex activation in pre-attentive change detection.
683 *Neuroimage*, 29(1), 314–20.
- 684 Tseng, Y.-L., Lu, C.-F., Wu, S.-M., Shimada, S., Huang, T., & Lu, G.-Y. (2018). A Functional
685 Near-Infrared Spectroscopy Study of State Anxiety and Auditory Working Memory Load. *Front*
686 *Hum Neurosci*, 12, e00313.
- 687 Verleger, R. (1988). Event-related potentials and cognition: A critique of the context updating
688 hypothesis and an alternative interpretation of P3. *Behav Brain Sci*, 11(3), 343–356.
- 689 Villringer, A., & Chance, B. (1997). Non-invasive optical spectroscopy and imaging of human brain
690 function. *Trends Neurosci*, 20(10), 435–42.
- 691 Walz, J. M., Goldman, R. I., Carapezza, M., Muraskin, J., Brown, T. R., & Sajda, P. (2013). Simulta-
692 neous EEG-fMRI reveals temporal evolution of coupling between supramodal cortical attention
693 networks and the brainstem. *J Neurosci*, 33(49), 19212–22.
- 694 Wolf, M., Wolf, U., Choi, J. H., Gupta, R., Safonova, L. P., Paunescu, L. A., et al. (2002). Functional
695 frequency-domain near-infrared spectroscopy detects fast neuronal signal in the motor cortex.
696 *Neuroimage*, 17(4), 1868–75.
- 697 World Medical Association. (2013). World Medical Association Declaration of Helsinki: ethical
698 principles for medical research involving human subjects. *JAMA*, 310(20), 2191–4.